Spin-polarization effects of an ultrarelativistic electron beam in an ultraintense two-color laser pulse

Huai-Hang Song,[1,4] Wei-Min Wang,[2,1,*] Jian-Xing Li,[3,†] Yan-Fei Li,[3] and Yu-Tong Li[1,4,5]

[1]*Beijing National Laboratory for Condensed Matter Physics, Institute of Physics, CAS, Beijing 100190, China*

[2]*Department of Physics and Beijing Key Laboratory of Opto-electronic Functional Materials and Micro–nano Devices, Renmin University of China, Beijing 100872, China*

[3]*MOE Key Laboratory for Nonequilibrium Synthesis and Modulation of Condensed Matter, School of Science, Xi'an Jiaotong University, Xi'an 710049, China*

[4]*School of Physical Sciences, University of Chinese Academy of Sciences, Beijing 100049, China*

[5]*Songshan Lake Materials Laboratory, Dongguan, Guangdong 523808, China*

(Received 2 May 2019; published 9 September 2019)

Spin-polarization effects of an ultrarelativistic electron beam head-on colliding with an ultraintense two-color laser pulse are investigated comprehensively in the quantum radiation-dominated regime. We employ a Monte Carlo method, derived from the recent work of Li *et al.* [Phys. Rev. Lett. **122**, 154801 (2019)], to calculate the spin-resolved electron dynamics and photon emissions in the local constant field approximation. We find that electron radiation probabilities in adjacent half cycles of a two-color laser field are substantially asymmetric due to the asymmetric field strengths and, consequently, after interaction the electron beam can obtain a total polarization of about 11% and a partial polarization of up to about 63% because of radiative spin effects, with currently achievable laser facilities, which may be utilized in high-energy physics and nuclear physics. Moreover, the considered effects are shown to be crucially determined by the relative phase of the two-color laser field and robust with respect to other laser and electron-beam parameters.

DOI: 10.1103/PhysRevA.100.033407

I. INTRODUCTION

As one of the intrinsic properties carried by electrons, spin has been extensively studied and utilized in high-energy physics [1–3], materials science [4], and plasma physics [5,6]. As known, the relativistic polarized electrons are commonly generated via two methods. The first extracts polarized electrons from a photocathode [7] or spin filters [8–10], and then employs a conventional accelerator or a laser wakefield accelerator [11] to accelerate them into the relativistic realm. The second directly polarizes a relativistic electron beam in a storage ring via using the radiative polarization effect (Sokolov-Ternov effect) [12–16]. However, the latter typically requires a long polarization time of minutes to hours because of the low static magnetic field at the Tesla scale.

Recently, the rapid development of ultrashort (with duration of approximately tens of femtoseconds) ultraintense (peak intensity $\approx 10^{22}$ W cm^{-2} and corresponding magnetic field $\approx 4 \times 10^5$ T) laser techniques [17,18] is providing opportunities to investigate electron polarization effects in such strong laser fields, analogous to the Sokolov-Ternov effect. Many theoretical works have been performed in nonlinear Compton scattering (e.g., see Refs. [19–23] and references therein). However, only a small polarization can be obtained in a monochromatic laser field [24] or a laser pulse [25]. A setup of strong rotating electric fields [26,27] shows a rather high polarization, when the electrons are trapped at the antinodes of the electric field. Unfortunately, this case may only occur for linearly polarized laser pulses of intensities $\gtrsim 10^{26}$ W cm^{-2} [28], which is much beyond current achievable laser intensities. Recently, a scheme with an elliptically polarized laser pulse has been proposed to split the electrons with different spin polarizations through spin-dependent radiation reaction [29] and, consequently, to reach a polarization above 70%. Also, a similar setup can be used to generate a positron beam with a polarization up to 90% due to asymmetric spin-dependent pair production probabilities [30].

Previous works indicate that the total polarization of all electrons in monochromatic laser pulses is negligible because of the symmetric laser field. In other words, asymmetric laser fields may result in a considerable polarization. The well-known asymmetric two-color laser configuration has been widely adopted in generation of terahertz radiation [31–34], high harmonic wave generation [35,36], and laser wakefield acceleration [37]. Recently, it is also proposed to generate polarized positron beams through multiphoton Breit-Wheeler pair production [38]. However, employing such two-color laser configuration to directly polarize the ultrarelativistic electron beam via nonlinear Compton scattering is still an open challenge.

In this paper, the polarization effects of an ultrarelativistic electron beam head-on colliding with a currently achievable ultraintense two-color laser pulse are comprehensively investigated in the quantum radiation-dominated regime (see the interaction scenario in Fig. 1). During the interaction, the radiation probabilities of electrons in the positive and negative half cycles of the two-color laser field are substantially asymmetric. Thus, after interaction considerable total polarization

*weiminwang1@ruc.edu.cn

†jianxing@xjtu.edu.cn

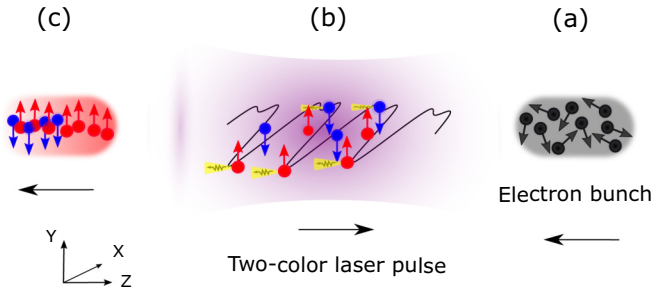

FIG. 1. The interaction scenario of an ultrarelativistic electron beam head-on colliding with an ultraintense two-color laser pulse. (a) An unpolarized electron beam propagates along the $-z$ direction, which can be obtained from a laser wakefield accelerator. (b) The interaction between the electron beam and the two-color laser pulse, polarizing along the x axis and propagating along the $+z$ direction, results in photon emissions and spin-flip transitions of the electrons. (c) A transversely polarized (in the y axis) electron beam can be achieved after interaction. The black-random (a), red-up (b), (c), and blue-down (b), (c) arrows indicate the unpolarized, spin-up, and spin-down electrons with respect to the $+y$ direction, respectively. The violet curve and the yellow signs with black lines in panel (b) indicate the two-color laser field and emitted photons, respectively.

and partial polarization can be obtained. We find that the relative phase ϕ of the two-color laser pulse is crucial to determine the polarization effects. In particular, when $\phi = \pi/2$, the laser field strengths in negative half cycles are much higher than those in the positive cycles, and, consequently, more photons of higher energies are emitted in the negative half cycles. Accordingly, the electron spins more probably flip to the direction antiparallel to the laser magnetic field in the electron's rest frame, assumed to be the instantaneous spin quantization axis (SQA) [29], and those electrons have lower remaining energies due to radiation-reaction effects [39]. As ϕ changes, the considered effects are weakened until complete disappearance in the case of $\phi = 0$. Moreover, the impacts of the laser and electron-beam parameters on the considered effects are studied, and optimal parameters are analyzed.

This paper is organized as follows. Section II presents the employed Monte Carlo simulation model. In Sec. III, the polarization effects of the ultrarelativistic electron beam in the two-color laser pulse are shown and analyzed, and the impacts of the laser and electron-beam parameters on the polarization effects are also investigated. Finally, a brief summary is given in Sec. IV.

II. THE THEORETICAL MODEL

The quantum electrodynamics (QED) effects in the strong field are governed by the dimensionless and invariant QED parameter $\chi \equiv (e\hbar/m^3c^4)\sqrt{|F_{\mu\nu}p^\nu|^2}$ [40], where $F_{\mu\nu}$ is the field tensor; p^ν is the electron's 4-momentum; and the constants $\hbar$, m, e, and c are the reduced Planck constant, the electron mass and charge, and the velocity of light, respectively. The normalized laser field amplitude parameter $\xi \equiv eE_0/(mc\omega_L) \gg 1$ and QED parameter $\chi \sim 1$ are considered to ensure that the coherence length of the photon emission is much smaller than the laser wavelength [40]. Here E_0 and ω_L are the laser field amplitude and angular frequency, respectively. The spin-dependent probability of photon emission in the local constant field approximation (LCFA) [40,41] can be written (summed up by photon polarization and electron spin after photon emission) as [25,29,42]

$$\frac{d^2\overline{W}_{\rm rad}}{dudt} = \frac{\alpha m^2c^4}{\sqrt{3}\pi\hbar\varepsilon_e}\left[\left(1-u+\frac{1}{1-u}\right)K_{2/3}(y) - \int_y^\infty K_{1/3}(x)dx - (\boldsymbol{S}_i\cdot\boldsymbol{\zeta})uK_{1/3}(y)\right], \quad (1)$$

where K_ν is the modified Bessel function of the order of ν, $y = 2u/[3(1-u)\chi]$, $u = \varepsilon_\gamma/\varepsilon_e$, ε_e is the electron energy before radiation, ε_γ is the emitted photon energy, and α is the fine-structure constant. The last term in Eq. (1) is a spin-dependent addition, where $\boldsymbol{S}_i$ is the initial spin vector of an electron before photon emission and $\boldsymbol{\zeta} = \boldsymbol{\beta}\times\hat{a}$. $\boldsymbol{\beta}$ is the electron velocity normalized by c, and $\hat{a} = \boldsymbol{a}/|\boldsymbol{a}|$ is the electron acceleration. The photon emission in a constant crossed field is discussed in Ref. [43], indicating that the electron spin $\boldsymbol{S}_i$ and $\boldsymbol{S}_f$ are along the magnetic field in the electron rest frame. By averaging over $\boldsymbol{S}_i$, the widely employed spin-averaged radiation probability can be obtained [44–48]. The spin vector $\boldsymbol{S} = (S_x, S_y, S_z)$, and $|\boldsymbol{S}| = 1$.

The stochastic photon emission by an electron can be calculated using the conventional QED Monte-Carlo algorithm [46] with a spin-dependent radiation probability given by Eq. (1). The electron dynamics in the external laser field is described by classical Newton-Lorentz equations, and its spin dynamics is calculated according to the Thomas-Bargmann-Michel-Telegdi equation [49–52]. After photon emission, the electron spin is assumed to flip either parallel or antiparallel to the instantaneous SQA (along $\boldsymbol{\zeta}$) with a probability given in Ref. [29]. Note that, as shown in the last term of Eq. (1), when the spin vector $\boldsymbol{S}_i$ is antiparallel to the instantaneous SQA, the electron has a higher probability to emit a photon.

Recently, the validity of the LCFA has been broadly discussed [43–48,53–58], and the LCFA is shown to be applicable when the parameter condition $\chi(1/u-1)/\xi^3 \ll 1$ is satisfied in the head-on colliding geometry [58]. In this paper, we employ the laser and electron-beam parameter conditions $\chi \sim 1$ and $\xi \sim 100$, and, therefore, the LCFA is applicable for emitted photon energies of $u = \varepsilon_\gamma/\varepsilon_e \gg 10^{-6}$. Note that the LCFA will break down when a dimensionless electron energy $b \sim 2(\hbar\omega_L\varepsilon_e)/m^2c^4 \gg 1$ [56,57]. Since GeV-level electron beams are used in this paper, b is at the level of 0.01 and the LCFA holds in our case.

III. RESULTS AND ANALYSIS

A. Simulation setup

In our simulations, the fundamental laser pulse of a wavelength $\lambda_0 = 1.0\,\mu$m and the second-harmonic pulse have the same duration, transverse profile, and linear polarization along the x direction. They propagate along the $+z$ direction and their combined electric field can be expressed as $E_x \propto [\xi_1\sin(\omega_L\eta) + \xi_2\ \sin(2\omega_L\eta + \phi)]$, where ξ_1 and ξ_2 are the normalized amplitudes of the fundamental and the second-harmonic pulses, respectively, $\eta = (t - z/c)$, and ϕ is the relative phase. We employ a three-dimensional description

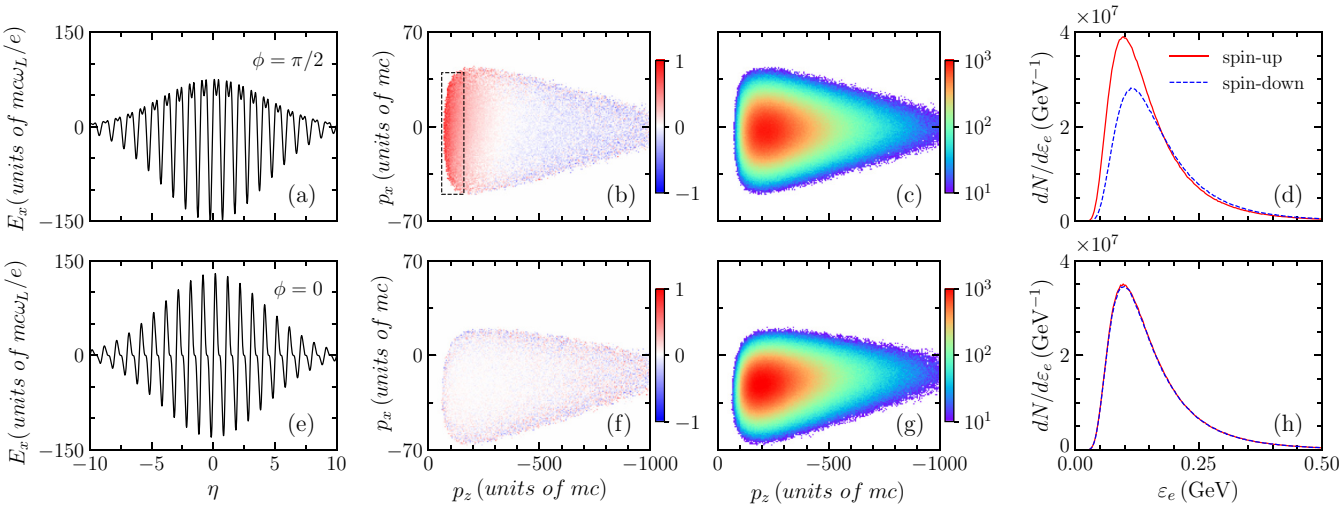

FIG. 2. (a), (e) The laser field E_x with respect to η. (b), (f) Distribution of the average polarization $\overline{S}_y$ vs longitudinal and transverse momenta p_z and p_x, respectively. (c), (g) Number density distributions of electrons vs p_z and p_x. (d), (h) Energy spectra of spin-up and spin-down electrons, respectively. Note that "spin-up" and "spin-down" indicate the electron spin parallel and antiparallel to the $+y$ axis, respectively. Upper panels (a)–(d) indicate the simulation results with $\phi = \pi/2$, and lower panels (e)–(h) indicate those with $\phi = 0$.

of the tightly focused laser pulse with a Gaussian temporal profile with the fifth order $(\sigma_0/z_r)^5$ in the diffraction angle [59], where $z_r = k_L\sigma_0^2/2$ is the Rayleigh length, $k_L = \omega_L/c$ is the wave vector, and σ_0 is the waist radius.

In our first simulation, we take the laser peak amplitude $\xi_1 = 2\xi_2 = 100$ (corresponding to the peak intensity $I_1 = 4I_2 = 1.37 \times 10^{22}$ W cm^{-2}), and full width at half maximum (FWHM) duration $\tau_0 = 10\ T_0$ (33 fs), where T_0 is the laser period. Considering the different Rayleigh lengths of two-color laser pulses, we first take the waist radius as infinity for simplicity, and then we will discuss the finite waist effects. Our simulations will show that the results in the plane-wave case are very close to the ones with $\sigma_0 \geqslant 5\,\mu$m. An unpolarized cylindrical electron beam is employed, including 10^7 electrons with initial mean energy $\varepsilon_0 = 2.0$ GeV (corresponding to the relativistic factor $\gamma_0 \approx 4000$), energy spread $\Delta\varepsilon_0/\varepsilon_0 = 10\%$, transversely Gaussian profile with a radius $r_1 = 3\,\mu$m, and longitudinally uniform profile with a length $r_2 = 5\,\mu$m. This kind of electron bunch can be obtained by laser wakefield accelerators [60,61]

During the head-on collision, one could assume the momenta of ultrarelativistic electrons to be approximately along the initial moving direction, i.e., the $-z$ direction, due to $\gamma_0 \gg \xi_1$. Hence, the magnetic fields experienced by the electrons in their rest frames are along the y axis. Note that "spin-up" and "spin-down" indicate the electron spin parallel and antiparallel to the $+y$ axis, respectively.

B. Electron polarization via radiative spin effects

The combined electric field of the two-color laser pulse has a highly asymmetric envelope profile in the positive and negative half cycles when $\phi = \pi/2$, as shown in Fig. 2(a). The electrons in the negative half cycles with higher field strengths have a larger QED parameter χ, which causes more photons with higher energies to be emitted than those in the positive half cycles. In the negative half cycles, the instantaneous SQA (along $\boldsymbol{\zeta} = \boldsymbol{\beta} \times \hat{a}$) is along the $-y$ direction; therefore, after photon emission the electron spin is more probably antiparallel to the SQA, i.e., the $+y$ direction [29]. This results in generation of more spin-up (with respect to the $+y$ direction) electrons, as shown in Fig. 2(d). Accordingly, the total polarization of the whole electron beam is about 11%. Moreover, due to radiation-reaction effects, more spin-up electrons have lower energies [see Fig. 2(b)]. In the region of $|p_z| < 160\,mc$ marked by the black dotted box, the polarization of 14% electrons is above 40%. Further, if one filters high-energy electrons, the polarization of remaining electrons with $|p_z| < 100\,mc$ is up to about 63%, as shown in Fig. 3. Obviously, the energy-dependent polarization could provide a way to generate a highly polarized electron beam by choosing electron energy. Also, it may present an experimental scheme to verify the theory of the spin-dependent radiation reaction. Note that the polarization of laser-driven ultrarelativistic

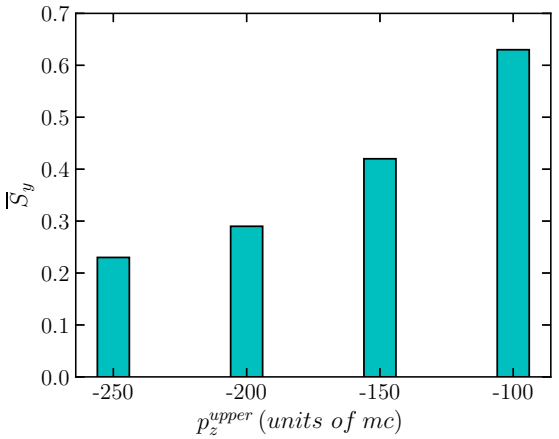

FIG. 3. The average polarization $\overline{S}_y$ of the electrons with different cutoff p_z.

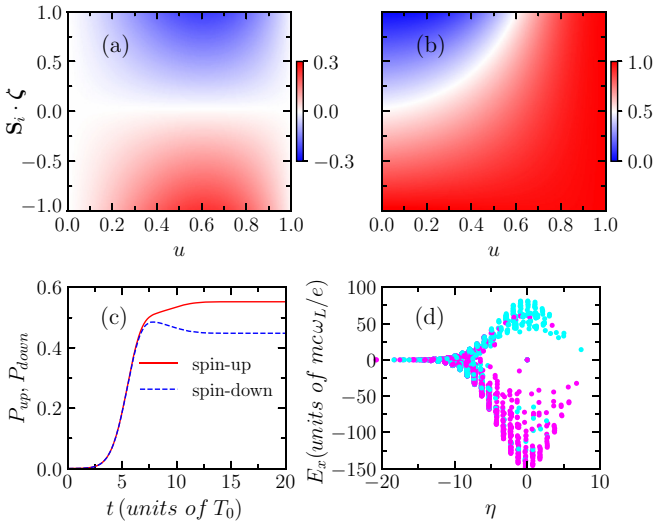

FIG. 4. (a) The ratio of the last term in Eq. (1) to the first two terms vs $\boldsymbol{S}_i \cdot \boldsymbol{\zeta}$ and u, where the QED parameter $\chi \approx 1.1$. (b) The probability that an electron spin flips to the direction antiparallel to the instantaneous SQA after emitting a photon, with $\chi \approx 1.1$. (c) Evolution of the proportions of the spin-up ($P_{\rm up}$, red solid line) and spin-down ($P_{\rm down}$, blue dotted line) electrons, respectively. (d) Tracks of spin-flip dynamics of 2000 electrons chosen randomly, where the violet and cyan points indicate electrons flipping to spin-up and spin-down, respectively, after photon emissions. Note that "spin-up" and "spin-down" indicate the electron spin parallel and antiparallel to the $+y$ axis, respectively. Other laser and electron parameters are the same as those in Fig. 2.

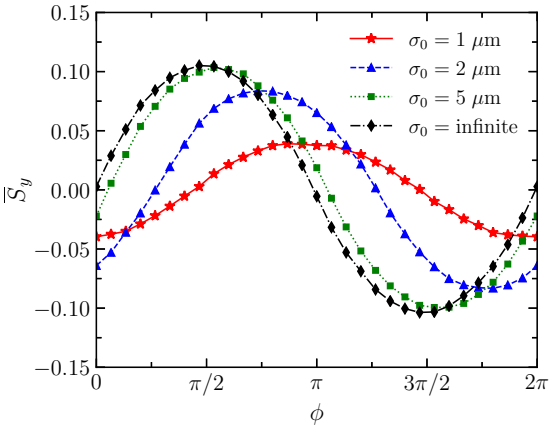

FIG. 5. The average polarization $\overline{S}_y$ as a function of the relative phase ϕ of the two-color laser pulse with different waist radii. Other laser and electron parameters are the same as those in Fig. 2.

electron beams can be measured via the polarimetry of nonlinear Compton scattering [62].

As $\phi = 0$, the combined electric field has symmetric envelope profiles in the positive and negative half cycles, as shown in Fig. 2(e). Such a laser field cannot generate more spin-up or spin-down electrons via nonlinear Compton scattering, as observed in Fig. 2(h), because the polarizations of electrons induced in the positive and negative cycles counteract each other. One can notice in Figs. 2(f) and 2(g) that the electrons can acquire a nonzero drift velocity in a such field configuration due to asymmetry in the laser vector potential [33,34] and radiation reaction [63]. Also, it is shown in Figs. 2(d) and 2(h) that the energy spectra of the spin-up and spin-down electrons both become broader compared with the initial quasimonoenergetic spectrum, because the electrons lose energies via stochastic photon emissions.

To analyze the reasons for the polarization effects, we show in Fig. 4 the details of the evolution of the electron-spin flips in the two-color laser field with $\phi = \pi/2$. When interacting with the laser field, electrons emit photons, and the spin flips either parallel or antiparallel to the instantaneous SQA [29]. The formed electron polarization can significantly affect the photon emission according to the last term in Eq. (1). With $\boldsymbol{S}_i \cdot \boldsymbol{\zeta} = -1$, i.e., the electron spin is antiparallel to the instantaneous SQA, the emission probability could be enhanced by about 30%; oppositely, it could be decayed by about 30% with $\boldsymbol{S}_i \cdot \boldsymbol{\zeta} = 1$, as shown in Fig. 4(a).

In Fig. 4(b), we demonstrate the probability that an electron spin flips to the direction antiparallel to the instantaneous SQA after emitting a photon. One can see that the spin-flip probability depends on both the electron-spin direction and the emitted photon energy. With $\boldsymbol{S}_i \cdot \boldsymbol{\zeta} < 0$, the electron spin very likely flips even though the emitted photon has a low energy. With $\boldsymbol{S}_i \cdot \boldsymbol{\zeta} > 0$, the spin flip arises with a high probability when the emitted photon energy is high enough. Basically, the electron spin tends to flip to the direction antiparallel to the SQA. Note that the above analysis holds at high laser intensities [$\chi \approx 1.1$ is employed in Figs. 4(a) and 4(b)]. When the laser intensity is low and the resulting QED parameter $\chi \sim \xi$ is also small, the photon energy is usually much lower than that of the electron, $u = \varepsilon_\gamma/\varepsilon_e \sim \chi$. Hence, contributions of the electron-spin term to the spin-flip probability as well as the radiation probability given by Eq. (1) can be ignored.

In Fig. 4(c), we show the ratios of the spin-up and spin-down electron numbers to the total electron number, respectively. When the electron beam collides with the rising edge of the laser pulse at $t \lesssim 7\,T_0$, the electrons gradually flip to spin-up or spin-down with nearly the same probability, due to the low laser field strength and small χ. As the electrons approach the laser pulse peak around $t \approx 10\,T_0$, more spin-up electrons are generated accompanied with higher-energy emitted photons. The similar results can be found in Fig. 4(d), in which we randomly choose 2000 electrons and track their dynamics. It is clearly shown that in the strong laser field region the spin flips are significant. In the negative half cycles of the electric field, the instantaneous SQA is along the $-y$ direction, and the electrons incline to flip to spin-up, i.e., the $+y$ direction. Oppositely, they tend to flip to spin-down, i.e., the $-y$ direction, in the positive half cycles. Because the field strengths in the negative half cycles are stronger, more electrons probably flip to spin-up, and, consequently, a polarized electron beam is obtained.

C. Impacts of the laser and electron-beam parameters on the total polarization of the electron beam

We further study the impacts of the laser and electron-beam parameters on the total polarization of the electron beam. In Fig. 5, we change the relative phase ϕ with different waist radius σ_0. When σ_0 approaches infinity, i.e., the plane-wave

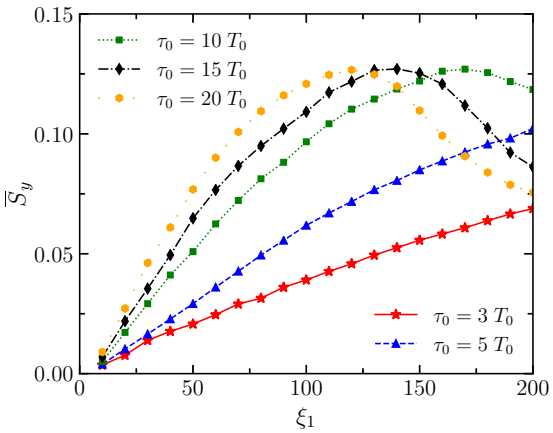

FIG. 6. The average polarization $\overline{S}_y$ as a function of ξ_1 with different pulse durations, where the initial electron energy $\varepsilon_0 = 2.0$ GeV. Here, $\sigma_0 = 5\mu$m is taken.

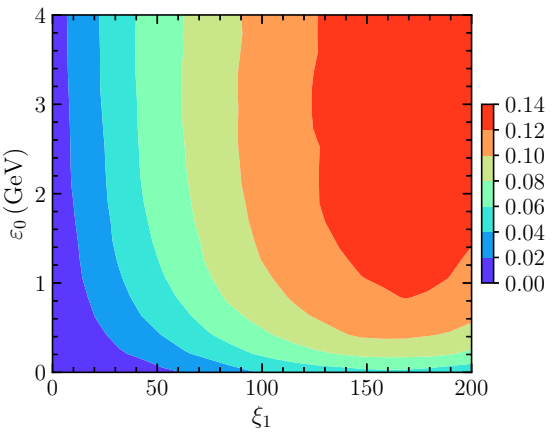

FIG. 7. The average polarization $\overline{S}_y$ vs the laser peak intensity and the initial electron energy ε_0. Here, $\tau_0 = 10\,\mathrm{T}_0$ and $\sigma_0 = 5\,\mu$m are taken.

case, shown by the black curve with diamonds, the total polarization is zero at $\phi = 0$, increases gradually to the maximum at $\phi = \pi/2$, and then decreases to zero at around $\phi = \pi$. Within the range of ϕ between π and 2π, the same result can be observed except that the polarization turns negative, i.e., more spin-down electrons are generated. This is because the laser strengths in the negative half cycles are higher with $\phi \in (0, \pi)$, while the ones in the positive half cycles are higher with $\phi \in (\pi, 2\pi)$. The dependency of the polarization on ϕ roughly follows the character of the function $\sin(\phi)$, similar to the THz generation dependency on ϕ [31], which results from the dependency of laser pulse envelope asymmetry between the positive and the negative half cycles on ϕ.

When we take the laser waist radius as $\sigma_0 = 5\,\mu$m, the dependency of the polarization on ϕ is still close to the plane-wave case. However, as the waist radius is further decreased to 2 and 1 μm, the dependency deviates gradually from the plane-wave case. The maximum of the polarization does not appear at $\phi = \pi/2$ and $3\pi/2$, and the maximum is reduced significantly. These characters can be explained by the different Rayleigh lengths between the fundamental laser pulse and the second-harmonic one. As the pulses propagate, the envelope of the combined laser field as well as the the ratio of two laser amplitudes walk off. They can remain the same as the plane-wave case only at the laser envelope peak. Therefore, the asymmetry of the laser field with $\phi = \pi/2$ is weakened with the decrease of the waist radius. To obtain a considerable polarization, the laser waist radius should be taken as $\sigma_0 \gtrsim 5\,\mu$m.

Furthermore, we investigate the impacts of the laser peak intensity and pulse duration on the considered effects, as presented in Fig. 6. We employ $\phi = \pi/2$, $\sigma_0 = 5\,\mu$m, and $\xi_1 = 2\xi_2$. When the laser duration $\tau_0 = 10\,T_0$ (FWHM $\sim$ 33 fs), with enhancing ξ_1 (as well as ξ_2) the polarization first increases and then decreases. Similar results are also observed with longer durations, e.g., $\tau_0 = 15\,T_0$ and $20\,T_0$. However, the peak appears at a lower ξ_1 for a longer duration. As the duration is decreased to $\tau_0 = 5\,T_0$ and $3\,T_0$, only a monotonical increase appears within the ξ_1 region considered. It is expected that the polarization will decay if higher ξ is adopted. One can also observe that in the increasing region the polarization is higher for a longer duration when the laser amplitude ξ_1 is fixed. The polarization first grows with both laser pulse duration and amplitude because of the probabilities of photon emission and electron-spin flip $\approx \chi\tau_0 \sim \xi\tau_0$. Due to photon emission, the electrons lose their energies. Provided the laser pulse duration is too long, the electrons could lose their main energies in the rising edge of the laser pulses, and the effective laser fields experienced by the electrons are much lower than that at the laser pulse peak. This could cause polarization decays with the increase of ξ_1.

Finally, we study the combined role of the initial electron energy ε_0 and the laser peak amplitude, as shown in Fig. 7. It is found that a high laser amplitude (e.g., $\xi_1 \gtrsim 100$) is necessary to obtain a high total polarization. With a high laser amplitude, the electron-beam energy could be flexible in a large range from hundreds of MeV to few GeV. On the other hand, even though a high electron-beam energy is taken (e.g., $\varepsilon_0 \approx 4$ GeV), the total polarization is relative low.

Note that a two-color laser pulse of multipetawatts required in our electron-spin-polarization scheme has become available recently [64,65]. For the typical laser parameters $\xi_1 = 100$, $\xi_2 = 50$, and $\sigma_0 = 5\,\mu$m used in our paper, the laser powers of the fundamental and second-harmonic components are 10.8 and 2.7 PW, respectively. Via a β-BaB_2O_4 (BBO) crystal [66], the second-harmonic one can be converted from a fundamental laser pulse with a power slightly higher than 2.7 PW since the conversion efficiency is high. Then, the generated second-harmonic laser pulse is automatically mixed with the remaining fundamental laser pulse with a power of 10.8 PW, where the two pulses coincide in both time and space. Note that a part of the fundamental one has been split to generate the second-harmonic one. This approach of the two-color field generation has been broadly adopted in terahertz generation experiments via a two-color laser scheme [31–33]. To avoid destroying the BBO crystal, the laser intensity should be lower than $10^{11}\,\mathrm{W\,cm^{-2}}$ on the crystal surface and, therefore, the size of the crystal is required to be at a meter level. Also, the two-color laser field can be focused to few micrometers in spot size to achieve the required high intensity. The relative phase

TABLE I. Dependency of the averaged polarization degree $\overline{S}_y$ on the colliding angle θ between two laser pulses if the two-color field is made from two quasimonochromatic pulses, where the simulation parameters are taken as the same as in Fig. 2 except for the laser waist radius $\sigma_0 = 5\,\mu$m used here.

Parameter	Value			
θ	0°	2°	5°	7°
$\overline{S}_y$	10.2%	9.9%	7.5%	5.7%

of the two-color laser field can be adjusted by placing a silicon wafer behind the BBO crystal. In addition, our simulations show in Table I that if the two-color field is made from two quasimonochromatic laser pulses superimposed on each other in experiments the angle between the two pulses should be small enough, e.g., below 2°, to avoid breaking the asymmetry of the two-color field.

IV. CONCLUSION

In summary, we have investigated the spin-polarization effects of an ultrarelativistic electron beam head-on colliding with an ultraintense two-color laser pulse. The asymmetry of the laser field in the processes of the photon emission and the electron-spin-flip transition causes considerable total and partial polarization. The polarization strongly depends on the relative phase ϕ of the two-color laser pulse. When $\phi = \pi/2$, the degree of a certain polarization reaches its peak. As ϕ is taken as $3\pi/2$, the same degree is achieved; however, the polarization turns opposite. Moreover, the spin-dependent radiation reaction results in the high polarization of relative-low-energy electrons, which provides a way to generate a highly polarized electron beam by choosing electron energy and may serve as a signature of the spin-dependent radiation reaction in the QED regime.

ACKNOWLEDGMENTS

This work was supported by the National Key R&D Program of China (Grant No. 2018YFA0404801), National Natural Science Foundation of China (Grants No. 11775302, No. 11874295, and No. 11804269), Science Challenge Project of China (Grant No. TZ2016005), and Strategic Priority Research Program of the Chinese Academy of Sciences (Grant No. XDB16010200).

[1] G. Moortgat-Pick, T. Abe, G. Alexander, B. Ananthanarayan, A. A.Babich, V. Bharadwaj, D. Barber, A. Bartl, A. Brachmann, S. Chen, J. Clarke *et al.*, Polarized positrons and electrons at the linear collider, Phys. Rep. **460**, 131 (2008).

[2] S. R. Mane, Yu. M. Shatunov, and K. Yokoya, Spin-polarized charged particle beams in high-energy accelerators, Rep. Prog. Phys. **68**, 1997 (2005).

[3] D. Abbott, P. Adderley, A. Adeyemi, P. Aguilera, M. Ali, H. Areti, M. Baylac, J. Benesch, G. Bosson, B. Cade *et al.* (PEPPo Collaboration), Production of highly polarized positrons using polarized electrons at MeV energies, Phys. Rev. Lett. **116**, 214801 (2016) .

[4] I. Žutić, J. Fabian, and S. Das Sarma, Spintronics: Fundamentals and applications, Rev. Mod. Phys. **76**, 323 (2004).

[5] M. Marklund and G. Brodin, Dynamics of Spin-$\frac{1}{2}$ Quantum Plasmas, Phys. Rev. Lett. **98**, 025001 (2007).

[6] G. Brodin and M. Marklund, Spin magnetohydrodynamics, New J. Phys. **9**, 277 (2007).

[7] D. T. Pierce and F. Meier, Photoemission of spin-polarized electrons from GaAs, Phys. Rev. B **13**, 5484 (1976).

[8] H. Batelaan, A. S. Green, B. A. Hitt, and T. J. Gay, Optically Pumped Electron Spin Filter, Phys. Rev. Lett. **82**, 4216 (1999).

[9] M. M. Dellweg and C. Müller, Spin-Polarizing Interferometric Beam Splitter for Free Electrons, Phys. Rev. Lett. **118**, 070403 (2017).

[10] M. M. Dellweg and C. Müller, Controlling electron spin dynamics in bichromatic Kapitza-Dirac scattering by the laser field polarization, Phys. Rev. A **95**, 042124 (2017).

[11] M. Wen, M. Tamburini, and C. H. Keitel, Polarized Laser-Wakefield-Accelerated Kiloampere Electron Beams, Phys. Rev. Lett. **122**, 214801 (2019).

[12] A. A. Sokolov and I. M. Ternov, Sov. Phys. Dokl. **8**, 1203 (1964).

[13] A. A. Sokolov and I. M. Ternov, *Synchrotron Radiation* (Akademic, Germany, 1968).

[14] V. N. Baier and V. M. Katkov, Radiational polarization of electrons in inhomogeneous magnetic field, Phys. Lett. A **24**, 327 (1967).

[15] V. N. Baier, Radiative polarization of electrons in storage rings, Sov. Phys. Usp. **14**, 695 (1972).

[16] Y. Derbenev and A. M. Kondratenko, Polarization kinematics of particles in storage rings, Zh. Èksp. Teor. Fiz. **64**, 1918 (1973).

[17] The Extreme Light Infrastructure (ELI), http://www.eli-beams.eu/en/facility/lasers/.

[18] Exawatt Center for Extreme Light Stidies (XCELS), http://www.xcels.iapras.ru/.

[19] P. Panek, J. Z. Kamiński, and F. Ehlotzky, Laser-induced Compton scattering at relativistically high radiation powers, Phys. Rev. A **65**, 022712 (2002).

[20] G. L. Kotkin, V. G. Serbo, and V. I. Telnov, Electron (positron) beam polarization by Compton scattering on circularly polarized laser photons, Phys. Rev. ST Accel. Beams **6**, 011001 (2003).

[21] D. V. Karlovets, Radiative polarization of electrons in a strong laser wave, Phys. Rev. A **84**, 062116 (2011).

[22] M. Boca, V. Dinu, and V. Florescu, Spin effects in nonlinear Compton scattering in a plane-wave laser pulse, Nucl. Instrum. Methods Phys. Res., Sect. B **279**, 12 (2012).

[23] K. Krajewska and J. Z. Kamiński, Spin effects in nonlinear Compton scattering in ultrashort linearly-polarized laser pulses, Laser Part. Beams **31**, 503 (2013).

[24] D. Yu. Ivanov, G. L. Kotkin, and V. G. Serbo, Complete description of polarization effects in emission of a photon by an electron in the field of a strong laser wave, Eur. Phys. J. C **36**, 127 (2004).

[25] D. Seipt, D. Del Sorbo, C. P. Ridgers, and A. G. R. Thomas, Theory of radiative electron polarization in strong laser fields, Phys. Rev. A **98**, 023417 (2018).

[26] D. Del Sorbo, D. Seipt, T. G. Blackburn, A. G. R. Thomas, C. D. Murphy, J. G. Kirk, and C. P. Ridgers, Spin polarization of electrons by ultraintense lasers, Phys. Rev. A **96**, 043407 (2017).

[27] D. Del Sorbo, D. Seipt, A. G. R. Thomas, and C. P. Ridgers, Electron spin polarization in realistic trajectories around the magnetic node of two counter-propagating, circularly polarized, ultra-intense lasers, Plasma Phys. Control. Fusion **60**, 064003 (2018).

[28] A. Gonoskov, A. Bashinov, I. Gonoskov, C. Harvey, A. Ilderton, A. Kim, M. Marklund, G. Mourou, and A. Sergeev, Anomalous Radiative Trapping in Laser Fields of Extreme Intensity, Phys. Rev. Lett. **113**, 014801 (2014).

[29] Y.-F. Li, R. Shaisultanov, K. Z. Hatsagortsyan, F. Wan, C. H. Keitel, and J.-X. Li, Ultrarelativistic Electron-Beam Polarization in Single-Shot Interaction with an Ultraintense Laser Pulse, Phys. Rev. Lett. **122**, 154801 (2019).

[30] F. Wan, R. Shaisultanov, Y.-F. Li, K. Z. Hatsagortsyan, C. H. Keitel, and J.-X. Li, Ultrarelativistic polarized positron jets via collision of electron and ultraintense laser beams, arXiv:1904.04305 (2019).

[31] K. Y. Kim, J. H. Glownia, A. J. Taylor, and G. Rodriguez, Terahertz emission from ultrafast ionizing air in symmetry-broken laser fields, Opt. Express **15**, 4577 (2007).

[32] V. A. Andreeva, O. G. Kosareva, N. A. Panov, D. E. Shipilo, P. M. Solyankin, M. N. Esaulkov, P. González de Alaiza Martínez, A. P. Shkurinov, V. A. Makarov, L. Bergé, and S. L. Chin, Ultrabroad Terahertz Spectrum Generation from an Air-Based Filament Plasma, Phys. Rev. Lett. **116**, 063902 (2016).

[33] L.-L. Zhang, W.-M. Wang, T. Wu, R. Zhang, S.-J. Zhang, C.-L. Zhang, Y. Zhang, Z.-M. Sheng, and X.-C. Zhang, Observation of Terahertz Radiation via the Two-Color Laser Scheme with Uncommon Frequency Ratios, Phys. Rev. Lett. **119**, 235001 (2017).

[34] W.-M. Wang, Z.-M. Sheng, Y.-T. Li, Y. Zhang, and J. Zhang, Terahertz emission driven by two-color laser pulses at various frequency ratios, Phys. Rev. A **96**, 023844 (2017).

[35] N. Dudovich, O. Smirnova, J. Levesque, Y. Mairesse, M. Yu. Ivanov, D. M. Villeneuve, and P. B. Corkum, Measuring and controlling the birth of attosecond XUV pulses, Nat. Phys. **2**, 781 (2006).

[36] M.-C. Chen, C. Mancuso, C. Hernández-García, F. Dollar, B. Galloway, D. Popmintchev, P.-C. Huang, B. Walker, L. Plaja, A. A. Jaroń-Becker, A. Becker, M. M. Murnane, H. C. Kapteyn, and T. Popmintchev, Generation of bright isolated attosecond soft X-ray pulses driven by multicycle midinfrared lasers, Proc. Natl. Acad. Sci. USA **111**, E2361 (2014).

[37] M. Zeng, M. Chen, L. L. Yu, W. B. Mori, Z. M. Sheng, B. Hidding, D. A. Jaroszynski, and J. Zhang, Multichromatic Narrow-Energy-Spread Electron Bunches from Laser-Wakefield Acceleration with Dual-Color Lasers, Phys. Rev. Lett. **114**, 084801 (2015).

[38] Y.-Y. Chen, P.-L. He, R. Shaisultanov, K. Z. Hatsagortsyan, and C. H. Keitel, Polarized positron beams via intense two-color laser pulses, arXiv:1904.04110 (2019).

[39] A. Di Piazza, C. Müller, K. Z. Hatsagortsyan, and C. H. Keitel, Extremely high-intensity laser interactions with fundamental quantum systems, Rev. Mod. Phys. **84**, 1177 (2012).

[40] V. I. Ritus, Quantum effects of the interaction of elementary particles with an intense electromagnetic field, J. Sov. Laser Res. **6**, 497 (1985).

[41] V. N. Baier, V. M. Katkov, and V. M. Strakhovenko, *Electromagnetic Processes at High Energies in Oriented Single Crystals* (World Scientific, Singapore, 1998).

[42] V. N. Baier, V. M. Katkov, and V. S. Fadin, *Radiation from Relativistic Electrons* (Atomizdat, Moscow, 1973).

[43] B. King, Double Compton scattering in a constant crossed field, Phys. Rev. A **91**, 033415 (2015).

[44] I. V. Sokolov, J. A. Nees, V. P. Yanovsky, N. M. Naumova, and G. A. Mourou, Emission and its back-reaction accompanying electron motion in relativistically strong and QED-strong pulsed laser fields, Phys. Rev. E **81**, 036412 (2010).

[45] N. V. Elkina, A. M. Fedotov, I. Yu. Kostyukov, M. V. Legkov, N. B. Narozhny, E. N. Nerush, and H. Ruhl, QED cascades induced by circularly polarized laser fields, Phys. Rev. ST Accel. Beams **14**, 054401 (2011).

[46] C. P. Ridgers, J. G. Kirk, R. Duclous, T. G. Blackburn, C. S. Brady, K. Bennett, T. D. Arber, and A. R. Bell, Modelling gamma-ray photon emission and pair production in high-intensity laser-matter interactions, J. Comput. Phys. **260**, 273 (2014).

[47] D. G. Green and C. N. Harvey, SIMLA: Simulating particle dynamics in intense laser and other electromagnetic fields via classical and quantum electrodynamics, Computer. Phys. Commun. **192**, 313 (2015).

[48] C. N. Harvey, A. Ilderton, and B. King, Testing numerical implementations of strong-field electrodynamics, Phys. Rev. A **91**, 013822 (2015).

[49] L. H. Thomas, The motion of the spinning electron, Nature (London) **117**, 514 (1926).

[50] L. H. Thomas, The kinematics of an electron with an axis, Philos. Mag. **3**, 1 (1927).

[51] V. Bargmann, L. Michel, and V. L. Telegdi, Precession of the Polarization of Particles Moving in a Homogeneous Electromagnetic Field, Phys. Rev. Lett. **2**, 435 (1959).

[52] M. W. Walser, D. J. Urbach, K. Z. Hatsagortsyan, S. X. Hu, and C. H. Keitel, Spin and radiation in intense laser fields, Phys. Rev. A **65**, 043410 (2002).

[53] M. Kh. Khokonov and H. Nitta, Standard Radiation Spectrum of Relativistic Electrons: Beyond the Synchrotron Approximation, Phys. Rev. Lett. **89**, 094801 (2002).

[54] A. Di Piazza, M. Tamburini, S. Meuren, and C. H. Keitel, Implementing nonlinear Compton scattering beyond the local-constant-field approximation, Phys. Rev. A **98**, 012134 (2018).

[55] A. Ilderton, B. King, and D. Seipt, Extended locally constant field approximation for nonlinear Compton scattering, Phys. Rev. A **99**, 042121 (2019).

[56] T. Podszus and A. Di Piazza, High-energy behavior of strong-field QED in an intense plane wave, Phys. Rev. D **99**, 076004 (2019).

[57] A. Ilderton, Note on the conjectured breakdown of QED perturbation theory in strong fields, Phys. Rev. D **99**, 085002 (2019).

[58] A. Di Piazza, M. Tamburini, S. Meuren, and C. H. Keitel, Improved local-constant-field approximation for strong-field QED codes, Phys. Rev. A **99**, 022125 (2019).

[59] Y. I. Salamin and C. H. Keitel, Electron Acceleration by a Tightly Focused Laser Beam, Phys. Rev. Lett. **88**, 095005 (2002).

[60] W. P. Leemans, A. J. Gonsalves, H.-S. Mao, K. Nakamura, C. Benedetti, C. B. Schroeder, C. Tóth, J. Daniels, D. E. Mittelberger, S. S. Bulanov, J.-L. Vay, C. G. R. Geddes, and E. Esarey, Multi-GeV Electron Beams from Capillary-Discharge-Guided Subpetawatt Laser Pulses in the Self-Trapping Regime, Phys. Rev. Lett. **113**, 245002 (2014).

[61] A. J. Gonsalves, K. Nakamura, J. Daniels, C. Benedetti, C. Pieronek, T. C. H. de Raadt, S. Steinke, J. H. Bin, S. S. Bulanov, J. van Tilborg, C. G. R. Geddes, C. B. Schroeder, C. Tóth, E. Esarey, K. Swanson, L. Fan-Chiang, G. Bagdasarov, N. Bobrova, V. Gasilov, G. Korn, P. Sasorov, and W. P. Leemans, Petawatt Laser Guiding and Electron Beam Acceleration to 8 GeV in a Laser-Heated Capillary Discharge Waveguide, Phys. Rev. Lett. **122**, 084801 (2019).

[62] Y.-F. Li, R.-T. Guo, R. Shaisultanov, K. Z. Hatsagortsyan, and J.-X. Li, Single-shot determination of spin-polarization for ultrarelativistic electron beams via nonlinear Compton scattering, Phys. Rev. Applied **12**, 014047 (2019).

[63] M. Tamburini, C. H. Keitel, and A. Di Piazza, Electron dynamics controlled via self-interaction, Phys. Rev. E **89**, 021201(R) (2014).

[64] C. Danson, D. Hillier, N. Hopps, and D. Neely, Petawatt class lasers worldwide, High Power Laser Sci. Eng. **3**, e3 (2015).

[65] SULF-10PW, http://news.sciencenet.cn/htmlnews/2017/10/392187.shtm.

[66] A. E. Kokh, T. B. Bekker, K. A. Kokh, N. G. Kononova, V. A. Vlezko, P. Villeval, S. Durst, and D. Lupinski, Nonlinear LBO and BBO crystals for extreme light sources, in *Proceedings of the 2010 International Conference on Advanced Optoelectronics and Lasers* (IEEE, Piscataway, 2010), pp. 127–129.